Squeezing of Oil-Swollen Surfactant Bilayers by a Membrane Protein

C. Nicot,[1] M. Waks,[1] R. Ober,[2] T. Gulik-Krzywicki[3], and W. Urbach[4]
[1]*Laboratoire d'Imagerie Paramétrique, Université Pierre et Marie Curie and URA 1458 CNRS, 15 rue de l'Ecole de Médecine 75270 Paris, Cédex 06, France*
[2]*Laboratoire de la Matière Condensée, Collège de France and URA 792 CNRS, 5 Place Marcellin Berthelot. 75231 Paris, Cédex 05, France*
[3]*Centre de Geńétique Moléculaire, UPR 2420 CNRS, 91190 Gif-sur-Yvette, France*
[4]*Laboratoire de Physique Statistique de l'École Normale Supérieure. URA 1306 CNRS, associated to Université Pierre et Marie Curie and Denis Diderot, 24 Rue Lhomond. 75231 Paris, Cédex 05, France*
(Received 2 May 1996; revised manuscript received 19 July 1996)

We have performed small angle x-ray scattering experiments on a ternary system made of a nonionic surfactant, dodecane, and water, in the absence and upon insertion of a transmembrane protein. In contrast to other proteins or polymers studied, its incorporation reduces the Bragg spacing from 200 Å to 80 Å, which scales as $c^{-0.5}$, where c is the protein surface density. The macromolecule incorporated into the hydrophobic part of the lamellar phase appears on freeze-fracture electron micrographs as intramembranous particles. The data are fitted by a simple model of thermally undulating lamellae decorated with protein molecules. [S0031-9007(96)01387-7]

PACS numbers: 87.22.Bt

Fluid membranes are observed when surfactants aggregate into extended bilayers, as in dilute L_α phases. The structure of these lyotropic liquid crystals has been described using neutron, light, and small angle x-ray scattering studies [1,2]. Among the various aspects of these biomimetic self-assemblies, their interaction with synthetic polymers has been documented [3,4]. In this respect peptides and furthermore proteins seem a more adequate experimental material since they are monodisperse, their size, sequence, and structure are also known. In the area of integral membrane proteins penetrating bilayers, data are scarce and especially information concerning protein-surfactant interactions remains crucial for the understanding of fundamental processes leading to the incorporation, the stability, and the active conformation of these macromolecules in liquid crystals. We report here the insertion of the Folch-Pi proteolipid, a water-insoluble transmembrane protein, into a smectic liquid crystalline phase (L_α). The protein has a molecular weight of 30 000 and constitutes the major protein of a highly specialized, multilamellar membrane: myelin of the central nervous system [5,6]. Recent two-dimensional models of the integral protein display four hydrophobic, membrane-spanning α-helices and several charged domains located in the interlamellar aqueous spaces [7,8]. The biological function of the proteolipid is not known, although a role in the preservation of the myelin sheath compaction has been proposed [9].

Nonionic surfactant systems constitute appropriate models for the study of membrane proteins in liquid crystal phases in the absence of long-range electrostatic interactions, held often responsible for protein destabilization [10]. Associations between the highly hydrophobic protein and the surfactant take place, provided hydrogen bonding or hydrophobic interactions are operative [11]. These forces play a crucial role in both the insertion mechanism and conformational stability of the membrane protein [12]. The ternary system, tetraethylene glycol monododecyl ether ($C_{12}E_4$)-water-dodecane, displaying a stable L_α phase at ambient temperature [13], has been selected to prevent a possible temperature denaturation of the protein. In such a system the multilayer membrane is composed of two surfactant monolayers surrounding the water layer and separated by the swelling dodecane (i.e., reverse lamellar phase) [14]. This Letter reports in what manner the incorporation of a transmembrane protein affects the L_α phase properties.

An excellent protein solubilization is achieved in the isotropic, homogeneous, optically clear reverse micellar solution at 30 °C [13], as attested by the ultraviolet absorption spectrum. The system transits to the L_α phase by simply lowering the temperature below the transition phase boundary. After a lag period (five days around 20 °C), an upper oil phase forms above the L_α protein-containing phase. Analysis confirms that oil is completely devoid of protein and contains the surfactant in an amount (determined by dry weight) corresponding to the free monomer concentration.

Freeze-fracture electron micrographs of L_α phase obtained as described elsewhere [15], depict a well-defined lamellar structure (Fig. 1). The surfaces visible on images are midsections through the hydrophobic part of the sample. In the absence of the protein, it displays the classical texture of dodecane [16]. When the protein is incorporated into the system, additional intramembrane particles appear. The concentration of these objects, calculated from images of the replicas, is in agreement with the number of protein monomers inserted into the samples, providing good evidence for the protein incorporation into the hydrophobic part of the lamellar phase.

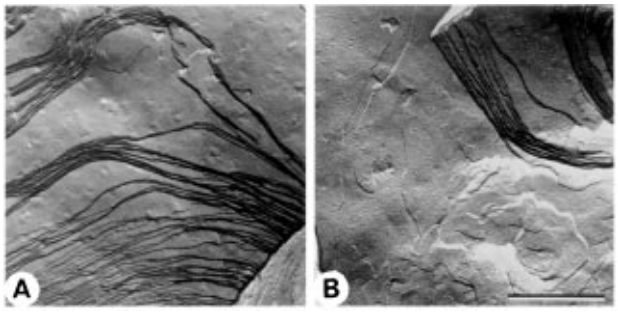

FIG. 1. Freeze-fracture electron micrographs of the L_α phases before (A) and after proteolipid incorporation (B). The volume fractions of the different system components are respectively $\Phi_{surf} = 0.49$, $\Phi_{water} = 0.18$, $\Phi_{oil} = 0.33$. The bar represents a length of 500 nm. Interlayer distance measured on the micrographs is in good agreement with SAXS data. The protein concentration of the sample is $2.35 \times 10^{-4} M$ and C, the protein-to-surfactant molar ratio, is 1.85×10^{-4}. Protein preparation as a precipitate in oil and its incorporation into the various phases are described in detail in Ref. [6].

To further characterize the system, small angle x-ray scattering (SAXS) [17] measurements were first performed in the absence of the protein at a constant (Φ_{water}/Φ_{surf}) ratio of 0.58 ± 0.01, used throughout the experiments (Φ is the volume fraction). The linear plot of the Bragg spacing d_B versus the inverse of the membrane volume fraction $\Phi_{memb} = \Phi_{surf} + \Phi_{water}$ in the 0.5–0.3 range, leads to a value of 50 ± 3 Å for the membrane thickness δ, according to the dilution law $d_B = \delta/\Phi_{memb}$, consistent with a simple geometric model of the lamellar phase (Nallet *et al.* [2]).

Figure 2 shows typical x-ray intensity scans of various L_α phases as a function of the scattering vector q. The solubilization of the proteolipid at a protein-to-surfactant molar ratio $C = 3.7 \times 10^{-4}$ induces, after the lag period, a large shift of the position of the wave vector peak q_0, indicating clearly a decrease of the Bragg spacing d_B, in comparison with the peak measured for the protein-free mixture. This result indicates that the protein has squeezed the lamellar phase. No such shift was detected after solubilization of water-soluble statistical polymers [4] or proteins, as shown for myelin basic protein on Fig. 2. The dramatic impact of the transmembrane protein incorporation on the liquid crystal phase is depicted in Fig. 3, showing that the decrease in the Bragg spacing d_B is dependent on the protein-to-surfactant molar ratio C since all the experimental points obtained at several Φ values gather on one single curve.

In the inset of Fig. 2, the spectrum of an L_α phase has been fitted to the Caillé model combining the membrane form factor and layer displacement thermal fluctuations [2,18]. We have used the line shape formula derived by Nallet, Laversanne, and Roux [2], which results from convolution of the thermally broadened peak for the finite size of well-oriented domains, with a Gaussian which

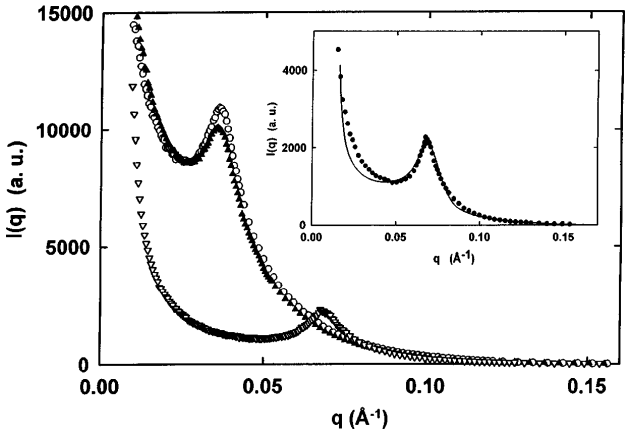

FIG. 2. Typical x-ray intensity scans of protein-free (▲) and proteolipid-containing (▽) L_α phases at a surfactant volume fraction $\Phi_{surf} = 0.18$ and at a protein-to-surfactant molar ratio C of 3.7×10^{-4}. Myelin basic protein (○) is at $C = 3.3 \times 10^{-4}$. From the peak position q_0 the Bragg distance $d_B = 2\pi/q_0$ is deduced. The x-ray small angle scattering experimental set-up has been described previously [17]. SAXS experiments have been performed on unoriented ("powder") samples. For these samples the tails of scattered peaks decay, according to the power law behavior $S(q) = |q - q_0|^p$ with p close to 1-η. The inset shows a fit of the spectrum of the proteolipid-containing L_α phase at $\Phi_{surf} = 0.18$ and at the protein-to-surfactant molar ratio $C = 3.3 \times 10^{-4}$. The fitted values are $\eta = 0.63$, $q_0 = 0.07$ Å^{-1}, and $\Delta q = 0.005$ Å^{-1} [2].

represents the experimental resolution and an additional line broadening due to the deformation of individual lamellae Δq. For values of $C < 3 \times 10^{-4}$ the small angle scattering is prevalent and the model is no more

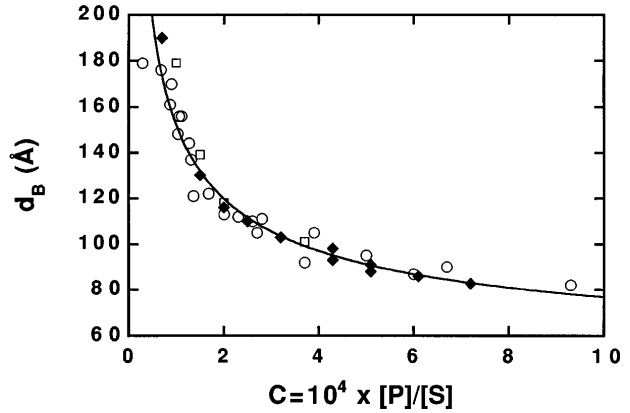

FIG. 3. Plot of the Bragg spacing obtained from the position of the maximum intensity Bragg peak q_0 as a function of protein-to-surfactant molar ratio C, measured at several different Φ_{surf} values 0.18 (○), 0.12 (□), and 0.08 (◆). For values of $C < 3 \times 10^{-4}$, small angle scattering has been taken into account for the determination of q_0 value. The drop in the Bragg distance reaches an asymptote around 80 Å, a value which is independent of the surfactant volume fraction. All experimental points gather on a single curve. The solid line is the fit by Eq. (2).

valid. For $C > 3 \times 10^{-4}$ the fitting parameters are the wave vector of the peak position q_0, Δq, and η the Landau-Peierls exponent [19,20], which is related to the bending rigidity constant of the lamella, κ, to the layer modulus for compression, $\overline{B}$, at constant chemical potential and to q_0:

$$\eta = \frac{q_0^2 k_B T}{8\pi\sqrt{K\overline{B}}}, \quad K = \frac{\kappa}{d_B}. \tag{1}$$

The fitted q_0 values were consistent with the values used in Fig. 3.

Now we consider the possible interpretation of the data presented in Fig. 3. Helfrich has shown that membrane spontaneous thermal fluctuations introduce a long-range entropic force, which stabilizes uncharged, swollen lamellar phases [20]. The mean interlamellar distance d_m is easily computed in the framework of harmonic approximation of membrane undulation. For a membrane with vanishing surface tension, the amplitude of thermal undulations is in order of a characteristic membrane dimension ξ and $d_m = A(T, \kappa)\xi$. The value of the parameter $A(T, \kappa)$ is model dependent [20,21].

We consider now a membrane decorated with proteins. Let ℓ be the mean distance between two neighboring proteins within a same lamella. Since the number of protein molecules incorporated within a single membrane is proportional to the total protein-to-surfactant ratio, the mean surface per protein is in order of $\ell^2 \approx c^{-1}$ (where c is the number of protein molecules per cm^2). As long as ℓ is $> \xi$, we can expect d_m to be independent of c. However, when c increases, ℓ becomes $\leq \xi$ then ℓ becomes the pertinent length and therefore $d_m = A(T, \kappa)\, c^{-0.5}$. This very rough model allows us to relate the repeat distance d_B obtained from the x-ray data to the membrane thickness δ and to the interlamellar distance d_m:

$$d_B = \delta + d_m = \delta + A(T, \kappa) c^{-0.5}. \tag{2}$$

The solid line drawn through the data of Fig. 3 results from a fit by Eq. (2) and illustrates the predictive capability of the model. In addition, an estimation of the membrane bending modulus κ can be extracted from the data [22]: $\kappa \approx 3k_B T$ and $\delta \approx 42 \pm 5$ Å, in good agreement with the value of δ as deduced previously from a plot of d_B vs Φ_{memb}.

Figure 4 illustrates the variation of $\eta^{0.5}$ as a function of $1/d_B$. The observed decrease of the value of η with $1/d_B$ is due to an increase of $K\overline{B}$ for the protein-containing bilayers. The interaction between bilayers induced by the protein is supported by visual observation of a gel-like behavior of the protein-containing L_α phase, not seen in a protein-free phase at an identical interlamellar distance d_m. Independent measurements of K and B could possibly be done on oriented samples to measure their dependence on protein concentration. However, presently, highly oriented L_α phase containing the protein is difficult to achieve. In Fig. 4, the data are fitted by the theoretical prediction of thermally stabilized bilayers [23]

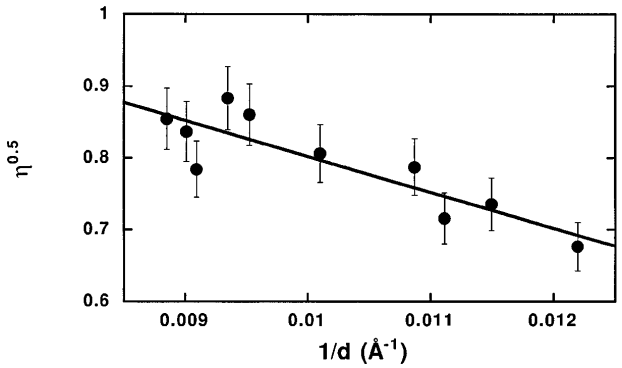

FIG. 4. Plot of the Landau-Peierls exponent η resulting from fits of the data $I(q)$ in the lamellar L_α phase. The straight line represents the fit of η according to the Helfrich theory, with $\eta^{0.5} = a\ (1\text{-}\delta/d_B)$, where d_B is the Bragg distance and δ the membrane thickness [23]. From the slope $\delta = 38 \pm 7$ Å is deduced.

$\eta = a(1 - \delta/d_B)^2$, where a is a constant on the order of 1. From the fit one gets $a = 1.14$ and $\delta = 38 \pm 7$ Å, in fair agreement with δ values determined above.

Finally, the behavior of lamellar phases after adsorption of macromolecules has been previously modeled [24,25]. Depending on concentration, the presence of attractive forces mediated by adsorbed, but not penetrating macromolecules, has been described to overcome the repulsive Helfrich interaction. Polymer confinement has also been described inside the bilayer of a lamellar phase controlled by Helfrich forces. A possible modification of the mechanical bilayer properties was observed by the investigators, but without any significative $d_B(C)$ dependence [4].

In the present report, in order to account for the observed $d_B(C)$ variations, we have used the Helfrich approach, where we have simply introduced a pertinent length related to the amount of the macromolecule added to the phase. Even if it agrees with our data, we are fully aware that the model is oversimplified. For example, the modifications of the membrane in the vicinity of the inclusion have not been accounted for. One interesting finding is that the biological macromolecule does not behave at all as statistical polymers do, even if they are included inside the bilayer [4]. One reason could be that these more flexible molecules spread over the bilayer on scales much larger than the persistence length of the membrane.

In contrast, the more rigid, spanning α-helices of the transmembrane proteolipid may induce a more localized membrane deformation, bringing two surfactant layers closer to each other. The squeezing process excludes most of the swelling oil, reduces the interlamellar distance, thus enabling the protein to establish links bridging two membranes. The final Bragg distance measured ($d_B = 80$ Å) represents an average value between the protein anchor points (the length of one α-helix is around 36 Å) and the maximum distance allowed for the membrane to fluctuate.

To the best of our knowledge, existing models cannot shed light on our results because they take into account macromolecules adsorbed on a bilayer, while in our experiments the macromolecule penetrates the bilayer. A more complete theoretical description is needed to define the complex interactions between macromolecules and membranes. In addition, our results stress the importance of hydrophobic interactions as the driving force for incorporation of hydrophobic helices into bilayers [12] and may constitute a model system for further studies. Ultimately, the squeezing of the interlamellar space may also mirror some of the biological properties of the proteolipid in maintaining the compact architecture of the native myelin sheath [9].

The authors would like to thank G. Gompper, J. Meunier, J. Prost, and P. Pincus for very stimulating discussions and A. Amarene for editorial help. This work was supported in part by l'Action Concertée "Interface Chimie, Physique, Biologie" du Ministère de l'Enseignement Supérieur et de la Recherche.

[1] C. R. Safinya, E. B. Sirota, D. Roux, and G. S. Smith, Phys. Rev. Lett. **62**, 1134 (1989); G. Porte, J. Marignan, P. Bassereau, and R. May, Europhys. Lett. **7**, 713 (1988).
[2] F. Nallet, R. Laversane, and D. Roux, J. Phys. II (France) **3**, 487 (1993).
[3] M. Singh, R. Ober, and M. Kleman, J. Phys. Chem. **97**, 11 108 (1993).
[4] E. Z. Radlinska, T. Gulik-Krzywicki, F. Lafuma, D. Langevin, W. Urbach, C. E. Williams, and R. Ober, Phys. Rev. Lett. **74**, 4237 (1995).
[5] M. B. Lees and S. W. Brostoff, in *Myelin,* edited by P. Morell (Plenum Press, New York, 1984), Chap. 6, p. 197.
[6] M. Vacher, M. Waks, and C. Nicot, J. Neurochem. **52**, 117 (1989).
[7] J. L. Popot, D. Pham Dinh, and A. Dautigny, J. Membrane Biol. **120**, 233 (1991).
[8] T. Weimbs and W. Stoffel, Biochemistry **31**, 12289 (1992).
[9] D. Boison, H. Bussow, D. D'Urso, H. W. Muller, and W. Stoffel, J. Neurosci. **15**, 5502 (1995).
[10] B. Honig and A. Nicholls, Science **268**, 1144 (1995).
[11] I. Iliopoulos and U. Olsson, J. Phys. Chem. **98**, 1500 (1994).
[12] J. J. Jones and L. M. Gierasch, Biophys. J. **67**, 1456 (1994).
[13] A. Merdas, M. Gindre, R. Ober, C. Nicot, W. Urbach, and M. Waks, J. Phys. Chem. **100**, 1518 (1996).
[14] H. Kunieda, K. Nakamura, H. T. Davis, and D. Fennel Evans, Langmuir **7**, 1915 (1991).
[15] T. Gulik-Krzywicki and J. Costello, J. Microscopy **112**, 103 (1978).
[16] W. Jahn and R. Strey, J. Phys. Chem. **92**, 2294 (1988).
[17] S. Giasson, D. Espinat, T. Palermo, R. Ober, M. Pessah, and M. F. Morizur, J. Colloid. Interface Sci. **153**, 355 (1992).
[18] A. Caillé, C. R. Acad. Sci. **B274**, 891 (1972); R. Zhang, W. Sun, S. Tristam-Nagle, R. L. Headrick, R. M. Sutter, and J. F. Nagle, Phys. Rev. Lett. **74**, 2832 (1995).
[19] R. E. Peierls, Annales Inst. Henri Poincaré **5**, 177 (1935); L. D. Landau, Phys. Z. Sowjetunion **2**, 26 (1937).
[20] W. Helfrich, Z. Naturforsch. **33A**, 305 (1978); W. Helfrich and R. M. Servuss, Nuovo Cimento Soc. Ital. Fis. **3D**, 137 (1984).
[21] F. Brochard and P. Lenon, J. Phys. (Paris) **36**, 1037 (1975); S. Leibler and R. Lipkowsky, Phys. Rev. B **35**, 7004 (1987).
[22] An extension of previous calculations was proposed to us by G. Gompper (private communication). Assuming $d_B^2 \approx \frac{k_B T}{\kappa} \int_{1/L}^{1/a} d^2q (q^4 + \ell^{-4})^{-1}$ and $\ell^2 = c^{-1}$, he obtains then $dm^2 = k_B T[\arctan(ca^2)^{-1} - \arctan(cL^2)^{-1}]/(2\kappa c)$. With $a = 40$ Å^2, the fit to this expression is equivalent to the fit of Eq. (2).
[23] D. Roux and C. R. Safinya, J. Phys. (Paris) **49**, 307 (1988).
[24] J. T. Brooks and M. E. Cates, J. Chem. Phys. **99**, 5467 (1993).
[25] G. Rossi and P. Pincus, Macromolecules **22**, 276 (1989).